Phase Conjugation of Optical Pulses in Fibers and in Semiconductor Laser Amplifiers

Sien Chi and Ying—Tso Lin
Institute of Electro—Optical Engineering,
National Chiao Tung University, Hsinchu, Taiwan, Republic of China.

Senfar Wen
Department of Electrical Engineering,
Chung—Hua Polytechnic Institute, Hsinchu, Taiwan, Republic of China.

Abstract

Temporal effects of the optical phase conjugation in dispersion—shifted fibers and in semiconductor laser amplifiers are numerically shown. In dispersion—shifted fibers, the frequency chirping is induced in the conjugate pulse by the signal pulse and pump wave through the cross—phase modulation, which increases with the signal power. In semiconductor laser amplifiers, the conjugate pulse has distortion and frequency chirping due to the amplified spontaneous emission noise and the carrier depletion induced by the signal pulse. These effects can be reduced by increasing the pump power. By proper choosing the signal power and pump power, for the both conjugators, the optical phase conjugations can be nearly ideal. Finally, the performances of the two conjugators are compared.

Keywords: optical phase conjugation, four—wave mixing, fiber, semiconductor laser amplifier

1. Introduction

The compensations of the pulse shape distortions due to the chromatic dispersion and Kerr effect by the optical phase conjugation (OPC) are recently demonstrated.[1-2] The idea to use the OPC to compensate the dispersion was proposed more than a decade ago.[3] It becomes an important issue because of the introduction of the erbium—doped fiber amplifier (EDFA). The operating wavelegnth of the EDFA is in 1550 nm band; while the dispersion in 1550 nm band is high for the standard fiber (STF) whose zero dispersion is in 1300 nm band. To compensate for the fiber loss with the EDFA without the expense of the bit rate, the fiber dispersion should be overcome. The conjugator can be made by utilizing the nearly degenerate four—wave mixing (NDFWM) in the dispersion—shifted fiber (DSF)[1] or in the semiconductor laser amplifier (SLA)[2]. In the DSF, the conjugate pulse is generated by the NDFWM due to the Kerr non—linearity, in which the pump wavelength is at the zero dispersion wavelength and the phase matching condition is satisfied. In the SLA, the conjugate pulse is generated by the NDFWM due to the nonlinear gain which mainly origniates from the intraband relaxation process occurring at a subpicosecond time scale and the signal wavelength is limited by the SLA gain bandwidth rather than by the phase matching condition. Recently, we have found that, in the DSF, there is frequency chirping in the conjugate pulse due to the cross—phase modulation (XPM) among the conjugate pulse, signal pulse, and pump wave, which may distort the pulse.[4] In the SLA, the conjugate pulse has distortion and frequency chirping caused by the carrier density depletion induced by the signal pulse.[5] In this paper, we will study the OPC pulses generated from the two conjugators and compare the performances of the two conjugators. The effect of the amplified spontaneous emission noise (ASEN) generated in the SLA on the conjugate pulse is considered.

2. Conjugator made by DSF

With the carrier $\exp[i(k_0 z - \omega_0 t)]$, where ω_0 is the carrier frequency and k_0 is the propagation constant at

0-8194-2156-1/96/$6.00

Downloaded From: http://proceedings.spiedigitallibrary.org/ on 05/01/2014 Terms of Use: http://spiedl.org/terms

ω_0. If ω_0 is the frequency at zero–dispersion, the complex envelope of the electric field propagating in the fiber can be written as[6]

$$i\frac{\partial\phi}{\partial z} - i\frac{1}{6}k_3\frac{\partial^3\phi}{\partial\tau^3} + \gamma|\phi|^2\phi = -\frac{1}{2}i\alpha\phi \,. \tag{1}$$

In Eq.(1), $\tau = t - z/v_g$ is the retarded time, where v_g is the group velocity; k_3 represents the third–order dispersion at ω_0; $\gamma = n_2\omega_0/cA_{eff}$, where n_2 is the Kerr coefficient and A_{eff} is the effective fiber cross section; α is the fiber loss. The term with γ in Eq.(1) is usually used to represent the self–phase modulation (SPM). In fact, it includes all the four–wave mixing (FWM) due to the Kerr non–linearity, for example, the XPM and OPC. To show these effects, we may decompose the electric field envelope as

$$\phi = \phi_p + \phi_s \exp(-i\Omega\tau) + \phi_c \exp(i\Omega\tau) \tag{2}$$

where ϕ_p is the pump wave with frequency $\omega_p = \omega_0$; ϕ_s and ϕ_c are the signal wave and the conjugate wave with frequencies $\omega_s = \omega_0 + \Omega$ and $\omega_c = \omega_0 - \Omega$, respectively. Since the slowly varying envelope approximation is assumed in deriving Eq.(1), it requires $|\Omega| << \omega_0$. Substituting Eq.(2) into Eq.(1) and neglecting the high frequency components, we have the equation for the conjugate for the conjugate wave

$$i\frac{\partial\phi_c}{\partial z} - \frac{1}{6}k_3\Omega^3\phi_c + i\frac{1}{2}k_3\Omega^2\frac{\partial\phi_c}{\partial\tau} + \frac{1}{2}k_3\Omega\frac{\partial^2\phi_c}{\partial\tau^2} - i\frac{1}{6}k_3\frac{\partial^3\phi_c}{\partial\tau^3}$$
$$+ \gamma[|\phi_c|^2 + 2|\phi_s|^2 + 2|\phi_p|^2]\phi_c + \gamma\phi_p^2\phi_s^* = -\frac{1}{2}i\alpha\phi_c, \tag{3}$$

where the terms with the time derivatives represent the dispersions of the fields. In Eq.(3), the terms represent the XPM are clearly seen. The last term in the left hand of Eq.(3) represents the FWM that is responsible for the OPC. In the followings, we take $k_3 = 7.4\times10^{-41}\text{sec}^3/\text{m}$, $n_2 = 3.2\times10^{-20}\text{m}^2/\text{W}$ and $A_{eff} = 50\ \mu\text{m}^2$.

The propagation of a Gaussian pulse is taken as an example, which is assumed to be

$$\phi_1 = \sqrt{P_1}\exp[-(\tau/\sigma_1)^2] \,, \tag{4}$$

where P_1 and σ_1 are its initial peak power and root–mean–square (rms) pulse width, respectively. The carrier wavelength $\lambda_s = 1542.9$ nm. It at first propagates in a 80 km–long STF with 0.22 dB/km loss and 16 ps/km/nm dispersion. The Kerr coefficient and effective fiber cross section of the STF are assumed to be the same as the DSF for simplicity. We take $P_1 = 1$ mW and $\sigma_1 = 70$ ps. At the end of the fiber, the pulse broadens and its pulse width becomes 83.13 ps. The pulse is then amplified to a peak power of P_2 and is launched into the DSF with zero dispersion wavelength $\lambda_0 = 1546.7$ nm and 0.24 dB/km fiber loss. The coupling loss is neglected for simplicity. The pump wave $\lambda_p = \lambda_0$ and with a power of P_p. Thus the initial condition used to solve Eq.(1) is

$$\phi = \sqrt{P_p} + \phi_2\exp(-i\Omega\tau) \,, \tag{5}$$

where the pump wave is continuous wave; ϕ_2 is the input signal pulse and Ω is the frequency deviation from the pump wave. Fig.1 shows the peak power of the conjugate pulse at $\lambda_c = 1550.5$ nm along the DSF for $P_p = 8$ mW and various signal powers P_2's. It is seen that the power of the conjugate pulse increases as the signal power and the optimum length is around 20 km, which agrees well with the experiments.[1] At the optimum length, the instantaneous frequencies $\delta\omega$ of the conjugate pulses with different P_2's are shown in Fig.2, where $\delta\omega = -\partial\psi/\partial\tau$ and ψ is the phase of the pulse. In Fig.2, the $\delta\omega$ of the input signal pulse is also shown for comparison. The frequency chirping of the input pulse is due to the chromatic dispersion and SPM in the STF. One can see that the $\delta\omega$ of the conjugate pulse is inverted with respect to the signal pulse. When P_2 is low, $\delta\omega$ is almost equal to the negative $\delta\omega$ of the input pulse. When P_2 is high, there is additional frequency chirping due to the XPM from the signal pulse and pump wave. The pulses broaden only slightly in the DSF because of low dispersion. After propagating 20 km in the DSF, the pulse widths of the conjugate pulses become 83.08, 83.23 and 84.46 ps for $P_2 = 0.1$, 1 and 8 mW, respectively; the peak powers of the conjugate pulses are 0.00214, 0.0212 and 0.156 mW for $P_2 = 0.1$, 1 and 8 mW, respectively. To compare with the input pulse width, there is almost no further pulse broadening in the DSF when P_2 is low. The broadening increases as the signal power because of the broadening of the signal pulse, which is enhanced by the frequency chirping due to the SPM because its wavelength is in the positive dispersion regime in the DSF. Because the group

Downloaded From: http://proceedings.spiedigitallibrary.org/ on 05/01/2014 Terms of Use: http://spiedl.org/terms

velocities of the signal and conjugate pulses are the same, there is no walk—off between the two pulses and the shape of the conjugate pulse follows the signal pulse. Therefore, to achieve an ideal conjugator, the signal power should be low and it is not desirable to use high signal power to amplify the conjugate pulse.

3. Conjugator made by SLA

The electric field of the optical wave propagating in the SLA is taken as $E(z,t)= \sqrt{2/A_m n_b \epsilon_0 c}\ \phi(z,t) \exp[i(k_0 z - \omega_0 t)]$, where A_m is the mode cross section and n_b is the refractive index. The field envelope ϕ is normalized so that the optical power $P=|\phi|^2$. The equations which govern the field propagating in the SLA can be written as[7-9]

$$\frac{\partial \phi}{\partial z} = \frac{1}{2}\Gamma a(N-N_0)[1-i\beta-\epsilon|\phi|^2]\phi - \frac{1}{2}\alpha_{int}\phi , \tag{6}$$

$$\frac{\partial N}{\partial \tau} = \frac{I}{qV} - \frac{N}{\tau_c} - \frac{a}{A_m h\nu}(N-N_0)(1-\epsilon|\phi|^2)|\phi|^2 . \tag{7}$$

In Eqs.(6) and (7), N is the carrier density; N_0 is the transparent carrier density; Γ is the confinement factor; a is the gain coefficient; β is the linewidth broadening factor; ϵ is the gain saturation coefficient; α_{int} is the internal loss coefficient; I is the injection current; q is the charge of a carrier; V is the active volume; τ_c is the carrier lifetime; $h\nu$ is the photon energy. In Eqs.(6) and (7), two sources of the NDFWM are included. One is caused by the carrier density modulation which is effective for the beat frequency up to about $1/\tau_c$. Typically, τ_c= 0.2—0.3 ns for the SLA and the bandwidth for the effective NDFWM is only few GHz. The other one is originated from the intraband relaxation process occurs at a much shorter time scale $\tau_i \cong$ 0.3 ps and the bandwidth for the effective highly NDFWM can be up to about 1 THz.[8] The complete treatment of this process should use the density matrix approach.[8] For simplicity, in Eqs.(6) and (7) we include the first order effect of the nonlinear compression of the optical gain by a factor $\epsilon|\phi|^2$, which is responsible for the spectral hole burning and highly NDFWM.[7-9] This model is valid when the beat frequency is much less than $1/\tau_i$ and the pulse width is much larger than τ_i. To show the phase conjugate wave generated from the carrier density modulation and nonlinear gain effect, we may decompose the field envelope as Eq.(2) and the carrier density as

$$N= N_S + \Delta N \exp(i\Omega\tau) + \Delta N^* \exp(-i\Omega\tau) , \tag{8}$$

where N_S is the slowly varying carrier density; ΔN is the fast varying carrier density which responds to the beat frequency. Substituting Eqs.(2) and (8) into Eqs.(6) and (7) and neglecting the high order terms, we have the equation for the conjugate wave

$$\begin{aligned}\frac{\partial \phi_c}{\partial z} =& \frac{1}{2}\Gamma a(1-i\beta)(N_S-N_0)\phi_c - \frac{1}{2}\alpha_{int}\phi_c \\ &- \frac{1}{2}\Gamma a(1-i\beta)(N_S-N_0)\gamma \frac{|\phi_p|^2\phi_c + \phi_p^2\phi_s^*}{1+\gamma(|\phi_p|^2+|\phi_s|^2+|\phi_c|^2)-i\Omega\tau_c} \\ &- \frac{1}{2}\Gamma a(N_S-N_0)\epsilon[(|\phi_c|^2+2|\phi_s|^2+2|\phi_p|^2)\phi_c+\phi_p^2\phi_s^*],\end{aligned} \tag{9}$$

where $\gamma = a\tau_c/A_m h\nu$. In the right hand of Eq.(9), the first term shows the gain from the carrier density; the third term and fourth term show the effects from the carrier density modulation and nonlinear gain effect, respectively, and the terms with $\phi_p^2\phi_s^*$ are the sources of the OPC. From Eq.(9), we can see that when the beat frequency is high the OPC from the carrier density modulation is reduced and the nonlinear gain effect is the dominate source for the OPC. In the followings, we take the typical numerical parameters for the SLA: Γ=0.4, a=2.5×10^{-16}cm^2, N_0=1×10^{18}cm^{-3}, α_{int}=40cm^{-1}, β=6, τ_c=0.25ns, amplifier length L=250μm, ctive—region width w=2μm, active—region depth d=0.2μm. V=Lwd and A_m=wd/Γ. For this amplifier structure, ϵ= 5.82W^{-1}.[8]

The signal pulse launched into the SLA is assumed to be the same as in the last section except its wavelength λ_S= 1551 nm. The pulse peak power in the SLA is P_2. The pump wavelength λ_p=1550 nm and the pump power in the SLA is P_p. Before the pump wave and active medium interact with the signal pulse

Downloaded From: http://proceedings.spiedigitallibrary.org/ on 05/01/2014 Terms of Use: http://spiedl.org/terms

(τ=—∞), the carrier density is saturated by the pump wave. The saturation density N_S can be easily obtained from Eq.(7) by taking $\partial N/\partial\tau$=0 and $|\phi|^2$=P_p. Eq.(5) and N=N_S are taken as the initial conditions for solving Eqs.(6) and (7).

Fig.3 shows the power envelopes of the conjugate pulses of wavelength λ_C= 1549 nm at the output of the SLA with I=250 mA and P_p=1 mW for P_2=0.1, 0.5, and 1 mW. In the figure, the power envelopes are normalized and the input signal pulse into the SLA is also shown for comparison. The peak powers of the output conjugate pulses are 0.0856, 0.255, and 0.298 mW for P_2= 0.1, 0.5 and 1 mW, respectively. One can see that, although the output power of the conjugate pulse increases as the input signal power, the pulse broadens and un—symmetrically distorts as the signal power increases. The rms pulse widths are 84.99, 92.19, and 100.5 ps for P_2= 0.1, 0.5, and 1 mW, respectively. From Eq.(9), because the gain is proportional to (N_S—N_0), the depletion of the slowly varying carrier density N_S by the signal pulse is responsible for the pulse shape distortion. For the case of P_2= 1mW shown in the Fig.3, the carrier density N in the SLA is shown in the Fig.4, where the fast varying carrier density ΔN responds to the beat frequency $\Omega/2\pi$= 125GHz. One can see that the leading edge of the conjugate pulse experiences more gain than the tailing edge and this leads to the un—symmetrical distortion. Furthermore, the central part of the conjugate pulse experiences less gain than the other parts of the conjugate pulse and this leads to the pulse broadening. Because the depletion of N_S increases as the signal power, the distortion of the conjugate pulse increases as the signal power. It is noticed that the contribution of the NDFWM from the carrier density modulation is small in these cases. If we assume ϵ=0, the output conjugate powers are reduced by about a factor of 10. As to the phase of the conjugate pulse, Fig.5 shows the instantaneous frequencies $\delta\omega$ for the conjugate pulses shown in the Fig.3. In the Fig.5, $\delta\omega$ of the input signal pulse is also shown for comparison, which is due to the chromatic dispersion and SPM in the STF. One can see that the $\delta\omega$ of the conjugate pulse is inverted chirping of the input signal pulse plus some additional frequency chirping. The additional frequency chirping comes from the phase modulation by the slowly varying carrier density N_S. Since the pulse shape distortion and additional frequency chirping come from the depletion of the carrier density, higher injection current provides higher gain but these two effects also increase. To reduce the pulse shape distortion and additional frequency chirping of the conjugate pulse, in addition to use low signal power, we may use high pump power to reduce the carrier density depletion induced by the signal pulse. However, when the signal power is low, we must consider the ASEN generated in the SLA.

The evolution of the ASEN power per unit frequency P_a in the SLA can be written as

$$\frac{dP_a}{dz} = [\Gamma a(N-N_0)(1-\epsilon P_t)-\alpha_{int}]P_a + \Gamma a N h\nu, \qquad (10)$$

where P_t is the average total optical power and the last term in Eq.(10) comes from the spontaneous emission. Including the ASEN, Figs. 6 and 7 show the power envelopes and instantaneous frequencies of the conjugate pulses, respectively, for the cases shown in Figs. 3 and 5. In Figs. 6 and 7, to clearly show the results, the ASEN has been filtered out by a 48 GHz ideal bandpass filter. To compare with Figs. 3 and 5, one can see that both the pulse shape and frequency chirping are distorted by the ASEN. Such distortions can also be reduced by increasing the pump power. Increasing the pump power compresses the gain of the SLA and the generated ASEN is reduced. To effectively reduce the distortions due to the ASEN and carrier depletion, the suitable signal power is about several tenths of milli—watts and the required pump power should be several milli—watts.

4. Comparison of the two conjugators

From the results shown in the last two sections, nearly ideal conjugator can be achieved by using either DSF or SLA. However, the quality for the phase conjugation is better by using the DSF. For example, Fig. 8 shows the instantaneous frequencies of the conjugate pulses at the output of the DSF and SLA, where for the both cases P_p= 8 mW and P_2= 0.5 mW. In Fig. 8, the corresponding rms pulse widths are 83.14 ps and 84.49 ps for the DSF and SLA, respectively; the corresponding peak powers are 0.011 mW and 0.198 mW for the DSF and SLA, respectively. It is noticed that, although in Fig.8 the same powers in the DSF and SLA are used, in fact the SLA requires higher pump power and signal power because the coupling loss from the fiber to the SLA is high (about 5.5 dB). From the section 2, the conversion efficiencies for the DSF is about —17

Downloaded From: http://proceedings.spiedigitallibrary.org/ on 05/01/2014 Terms of Use: http://spiedl.org/terms

dB. From the ref.1, the experimental result is −25.1 dB. In the section 2, the following assumptions are taken: (1) the polarizations of the signal and pump waves are the same, (2) $\lambda_p=\lambda_0$ and λ_0 does not change along the fiber. The different conversion efficiencies obtained from the theory and the experiment may come from the invalidities of the assumptions in practice and different fiber parameters. From the section 3, the conversion efficiencies for the SLA is about −14.5 dB (including 11 dB coupling loss), which is close to the −12.5 dB experimental result obtained in the ref.2, although the experimental conditions are different from the section 2. From the experimental results, the conversion efficiency of the DSF is much lower than the SLA. As the conjugate pulse must be amplified so as to further propagate in the STF, the optical amplifier (e.g. EDFA) following the conjugator made by the DSF requires higher gain and introduces more ASEN.

5. Conclusions

Generations of the conjugate pulses in DSF and in SLA are numerically shown, respectively. In DSF, the frequency chirping of the conjugate pulse due to the signal pulse and pump wave through the XPM in the DSF is shown. The frequency chirping decreases as the signal power. In SLA, the pulse shape distortion and frequency chirping of the conjugate pulse due to the ASEN and the carrier density depletion induced by the signal pulse in the SLA are shown. Both effects can be reduced by increasing the pump power to compress the gain and reduce the carrier density depletion. By proper choosing the signal power and pump power, for the both conjugators, the optical phase conjugations can be nearly ideal. Finally, the performances of the two conjugators are compared.

5. References

1. S. Watanabe, T. Naito, and T. Chikama," Compensation of chromatic dispersion in a single—mode fiber by optical phase conjugation," IEEE Photon. Technol. Lett., Vol. 5, pp.92—95, 1993.

2. M.C. Tatham, G. Sherlock, and L.D. Westbrook," Compensation fiber chromatic dispersion by optical phase conjugation in a semiconductor laser amplifier," Electron. Lett., Vol. 29, pp. 1851—1852 , 1993.

3. A. Yariv, D. Fekete, and D. M. Pepper," Compensation for channel dispersion by nonlinear optical phase conjugation," Opt. Lett., Vol. 4, pp. 52—54, 1979.

4. S. Wen, S. Chi, and T.—C. Chang," Effect of cross—phase modulation on optical phase conjugation in dispersion—shifted fiber," Opt. Lett., Vol. 19, pp. 939—941, 1994.

5. S. Wen and S. Chi," Effect of carrier depletion on optical phase conjugation in a semiconductor laser amplifier," Opt. Lett., Vol. 20, pp. 590—592, 1995.

6. G. P. Agrawal," Nonlinear fiber optics," 1st ed., pp. 40, Academic Press, Boston, 1989.

7. T. L. Koch and R. A. Linke, " Effect of nonlinear gain reduction on semiconductor laser wavelength chirping," Appl. Phys. Lett., Vol. 48, pp. 613—615, 1986.

8. G. P. Agrawal," Population pulsations and nondegenerate four—wave mixing in semiconductor lasers and amplifiers," J. Opt. Soc. Am. B, Vol. 5, pp. 147—158, 1988.

9. K. Kikuchi, M. Kakui, C.—E. Zah, and T.—P. Lee," Observation of highly nondegenerate four—wave mixing in 1.5μm traveling—wave semiconductor optical amplifiers and estimation of nonlinear gain coefficient," IEEE J. Quantum Electron., Vol. 28, pp. 151—156, 1992.

Downloaded From: http://proceedings.spiedigitallibrary.org/ on 05/01/2014 Terms of Use: http://spiedl.org/terms

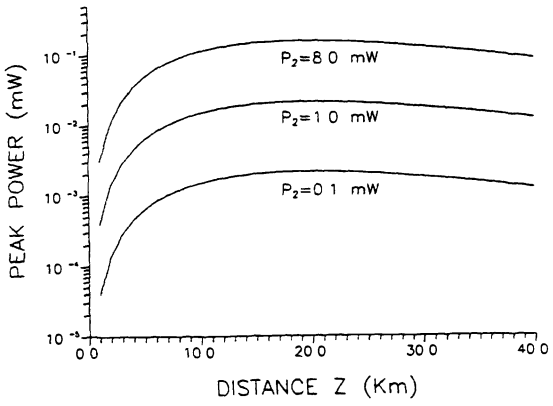

Figure 1: Peak powers of the conjugate pulses along the DSF for 8 mW pump power and various signal powers P_2's.

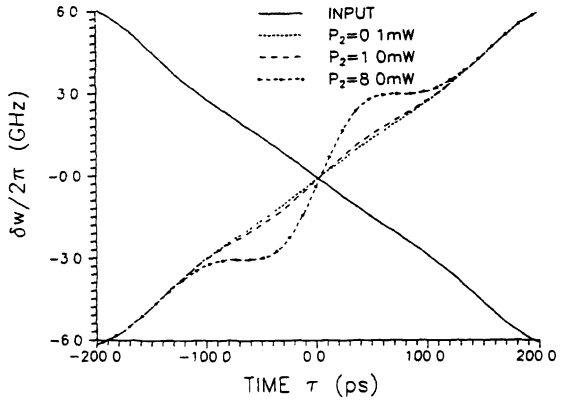

Figure 2: Instantaneous frequencies $\delta\omega$ of the conjugate pulses after propagating 20 km in the DSF for the cases shown in Fig.1. The $\delta\omega$ of the input signal pulse is also shown.

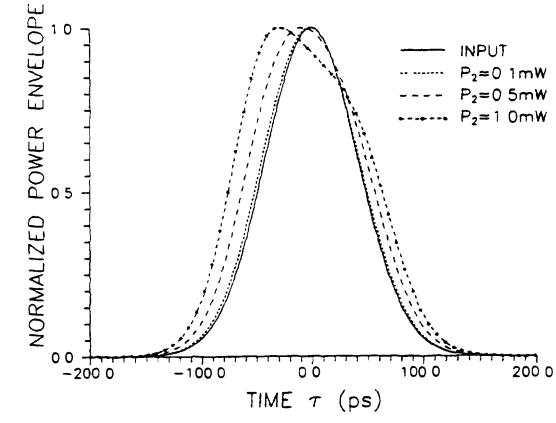

Figure 3: Normalized power envelopes of the conjugate pulses at the output of the SLA without ASEN for the signal power P_2= 0.1, 0.5 and 1 mW. The pump power P_p= 1 mW. The input power envelope of the signal pulse into the SLA is also shown for comparison.

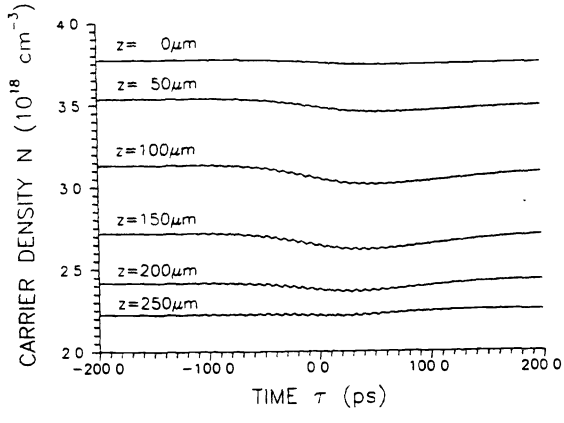

Figure 4: Carrier density N in the SLA for the case of signal power P_2= 1mW shown in the Fig.3. The corresponding distance z is shown near the data line.

Downloaded From: http://proceedings.spiedigitallibrary.org/ on 05/01/2014 Terms of Use: http://spiedl.org/terms

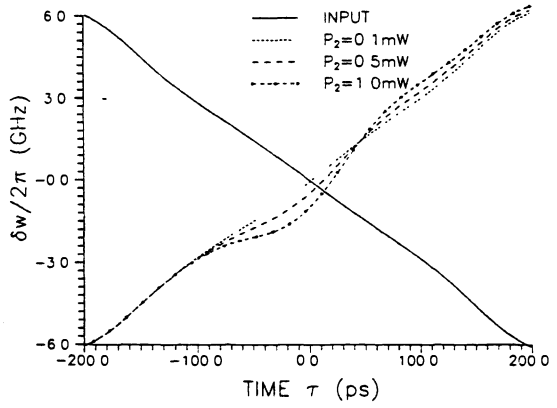

Figure 5: Corresponding instantaneous frequencies $\delta\omega$ of the output conjugate pulses and input signal pulse shown in the Fig.3.

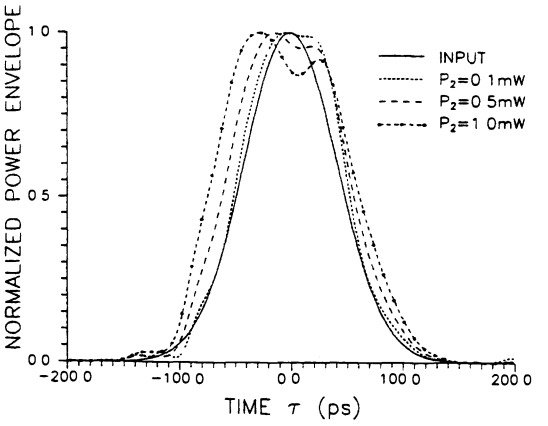

Figure 6: Normalised power envelopes of the conjugate pulses at the output of the SLA with ASEN for the signal power P_2= 0.1, 0.5 and 1 mW. The pump power P_p= 1 mW. The input power envelope of the signal pulse into the SLA is also shown for comparison.

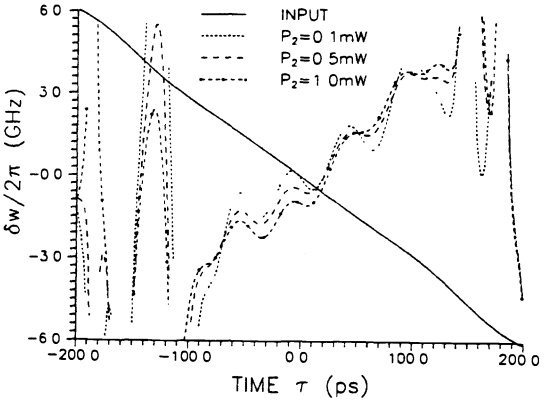

Figure 7: Corresponding instantaneous frequencies $\delta\omega$ of the output conjugate pulses and input signal pulse shown in the Fig.6.

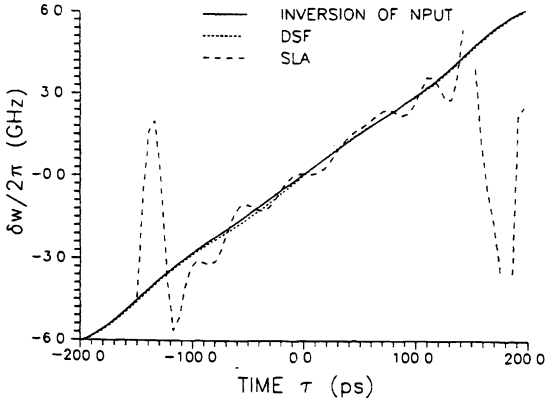

Figure 8: Instantaneous frequencies $\delta\omega$ of the conjugate pulses at the output of DSF and SLA for P_p= 8 mW and P_2= 0.5 mW. The inverted instantaneous frequency $-\delta\omega$ of the input signal pulse is also shown. The length of DSF is 20 km.

Downloaded From: http://proceedings.spiedigitallibrary.org/ on 05/01/2014 Terms of Use: http://spiedl.org/terms